Journal of
Mechanical
Science and
Technology

Journal of Mechanical Science and Technology 21 (2007) 771~777

Effect of Boron Contents on Weldability in High Strength Steel

H. W. Lee[a,*], Y. H. Kim[a], S. H. Lee[a], S. K. Lee[a], K. H. Lee[b], J. U. Park[c], J. H. Sung[a]

[a]*Department of Materials Science and Engineering, Dong-A university, Busan, Korea*
[b]*Korea Institute of Machinery & Materials, Changwon, Gyungnam, Korea*
[c]*Department of Civil Engineering, Chosun university, Gwangju, Korea*

(Manuscript Received June 1, 2006; Revised March 22, 2007; Accepted March 23, 2007)

Abstract

Three experimental flux cored wires(basic type) designed to produce systematic variations in the concentrations of boron of 32 ppm, 60 ppm and 103 ppm in the weld metal were prepared. A previous study of crack properties, morphology and microstructure in accordance with welding conditions was published in Welding Journal(Lee, 2006). Microstructure, strength and absorbed energy were studied for EH32 TMCP (Thermo-Mechanical Controlled Process) 40 mm thick plate welded with a gas-shielded flux cored arc welding.

The volume fraction of acicular ferrite decreased with increasing boron contents 32 to 103 ppm. The upper bainite instead of acicular ferrite was formed in the 103 ppm boron weld metal. The hardness values welded with 32 ppm and 60 ppm boron wire welds were in the range of Hv 190~210, while those welded with 103 ppm boron wire weld were in the range of Hv 230~235.

The absorbed energy slightly decreased with increasing boron contents from 32 ppm to 60 ppm, but significantly decreased with increasing boron contents from 60 ppm to 103 ppm. In the weld joint welded with 32 ppm and 60 ppm boron content electrode, no cracks were detected. However, cracks were detected the specimen welded with 103 ppm boron content electrode.

Keywords: Boron contents; Weld crack; Bainite; Acicular ferrite; Hardenability

1. Introduction

The mechanical properties of welds are related to carbon equivalents(Ceq), composition of the welds, heat input(cooling rate), and prior austenite grain size and so on. For a given steel composition, a faster weld cooling will lead to harder microstructural constituents such as bainite and martensite. In contrast, a slower cooling will lead to soft ferritic microstructures(Babu, et al., 1998).

A small content of boron in the weld metal affects the mechanical properties, such as its microstructure, hardness, strength, and absorbed energy. The amount of acicular ferrite, which is beneficial to impact toughness, in the weld metal is a very important factor to be considered. Acicular ferrite is reduced as boron content is increased. This is due to the decrease of eutectoid temperature. Finally bainite, material of low temperature transformation, is more easily formed (Melloy, 1973; Brown, 1974; Llewellyn, 1974).

Nickel is used in welds to increase the low-temperature notch toughness without increasing tensile strength higher than actually needed. Several investigators discovered that the addition of a combination of titanium and boron into a welded metal effectively produces a fine acicular ferrite microstructure(Koukabi,

*Corresponding author. Tel.: +82 51 200 7752, Fax.: +82 51 200 7759
E-mail address: hwlee@dau.ac.kr

1975; kohno, 1982). Various mechanisms have been proposed for boron hardenability in steels. One suggestion for boron hardenability is based on the fact that free boron diffuses to the austenite grain boundaries to lower their energy, thereby making them less favorable sites for ferrite nucleation(Maitrepierre 1975).

Koukabi, et al.(1975) have reported that microstructures consisting primarily of acicular ferrite provide the optimum weld metal mechanical properties, both in strength and toughness. Large volume fractions of upper bainite, side-plate ferrite, and grain boundary ferrite are considered detrimental to toughness.

To control the weld metal acicular ferrite content, researchers have introduced welding consumables containing alloying elements.

This study characterizes the effects of boron on the microstructure and mechanical properties in the deposited weld metal welded with three experimental flux cored wires designed to produce systematic variations in the concentrations of boron of 32 ppm, 60 ppm and 103 ppm.

2. Experimental procedures

2.1 Test panel

The size of the test panel was 2,000 mm long x 1,800 mm wide x 40 mm thick. The panel was fabricated from EH32 TMCP high strength hull steel.

Three sets of test panels of the same size and morphology were made, as shown in Fig. 1, and were welded in multi layers, as shown in Fig. 2.

2.2 Welding

Three experimental flux cored wires(basic type) designed to produce systematic variations in the concentrations of the weld metal boron of 32 ppm, 60 ppm and 103 ppm controlled by Ti-Ni addition were prepared. The panel was made with three electrodes, by the flux cored arc welding process with an automatic carriage (1.4 mm diameter, 20 L/min. flow rate, 100% CO_2 gas, electrode extension of 25~30 mm). Welding parameters are shown in Table 1.

2.3 Chemical composition

The chemical analyses of base metal and three welds were performed with a Baird Emission Spectrometer. The weld metal oxygen, and nitrogen con-

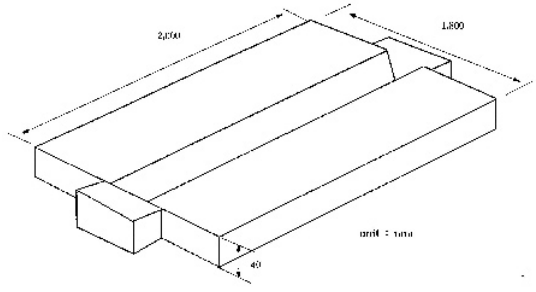

Fig. 1. Schematic diagram of weld panel.

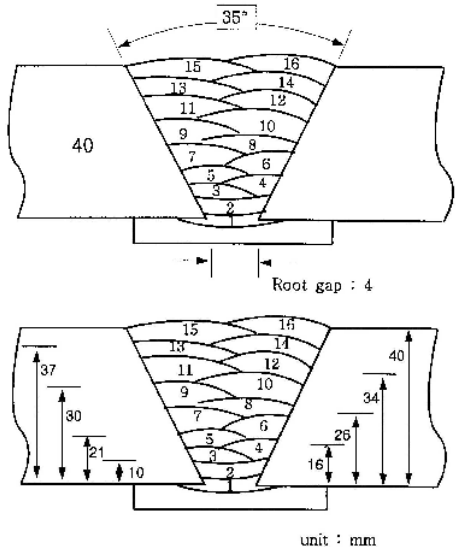

Fig. 2. Schematic diagram of weld deposit metal.

Table 1. Welding parameters.

Pass No.	Current (A)	Voltage (V)	Travel Speed (cpm)	Heat input (KJ/cm)
1-2	260	28	18	24
3-7	320	30	25	23
8-14	330	32	25	25
15-16	320	31	22	27

Welding process	Flux cored arc welding
Welding position	Flat
Filler metal specification	A 5.29 E81T1-K2
Filler metal classification	DS 81-K2
Shielding gas/ flow rate	CO_2 (100%)
Electrode extension (mm)	25-30
Polarity	DCRP
Preheating/ interpass temp.	50℃

Table 2. Chemical composition of base metal.

	C	Si	Mn	P	S	Ni	Cr	Mo	V	Ti	TS (N/mm^2)	YS (N/mm^2)	EI (%)
EH32 TMCP (spec.)	0.18 max.	0.10 ~0.50	0.90 ~1.60	0.040 max.	0.040 max.	0.04 max.	0.02 max.	0.08 max.	0.10 max.	0.02 max.	440~590	310 min.	20.0
Base metal (experi.)	0.08	0.38	1.35	0.015	0.005	0.03	0.03	0.02	0.002	0.02	518	372	31.0

Table 3. Chemical composition of weld metals.

	C (wt%)	Si (wt%)	Mn (wt%)	P (wt%)	S (wt%)	Ni (wt%)	Ti (wt%)	B (ppm)	O (ppm)	N (ppm)
No. 1	0.02	0.55	1.41	0.010	0.006	1.85	0.050	32	284	126
No. 2	0.02	0.54	1.38	0.012	0.005	1.90	0.045	60	290	134
No. 3	0.02	0.54	1.40	0.010	0.005	1.87	0.048	103	276	142

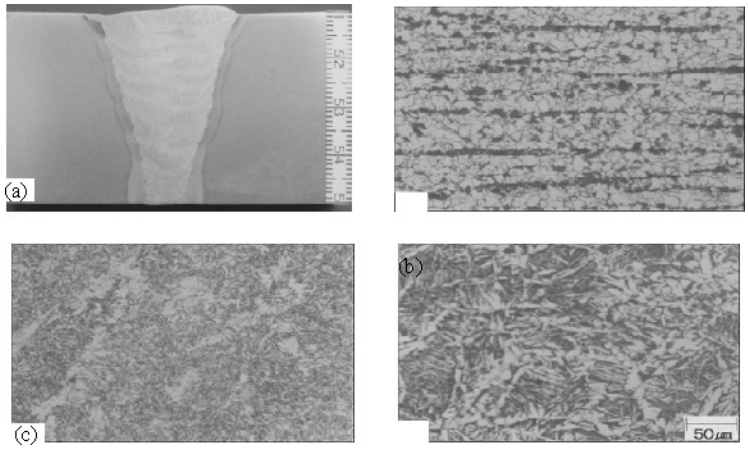

(a) Macrostructure of weld joint (b) Microstructure of base metal
(c) Deposit metal (d) Grain-coarsened zone
Fig. 3. Macro/microstructure of weld joint.

tents were determined using Leco Interstitial Analyzers. Chemical composition of base and weld metals are shown in Table 2 and Table 3 respectively. All other their composition of the alloy, except for boron, were constant.

2.4 Microstructure and mechanical properties

The specimens were prepared by polishing with a one micron alumina abrasive and then by etching for 10-15s in a solution of 2% Nital. A standard point counting technique was used to determine the volume fractions of acicular ferrite in the weld at a magnification of 500 x. The microstructural constituents were classified based on the guidelines suggested by Pargeter and Dolby(1985).

The tensile test was carried out at room temperature with round type standard specimen [12.7 mm(D), 50 mm(G), 58 mm(A), 9.5 R] by ASTM E8. The specimens from all deposit metal were made. Hardness was measured by using the macro Vickers hardness test, with a load of 5 kg and 10 s of loading time. Measurements were made on the transverse section at 20mm from the top surface. Impact test was performed at 20, 0, and -20℃ using Charpy V-notch specimen(10 mm × 10 mm × 55 mm) for the deposited metal by ASTM E23. The notch was machined the center of all weld metal.

3. Result and discussion

3.1 Macro/Microstructure

The macrostructures of weldments are shown in Fig. 3(a). Some significant differences can be noted between the heat affected zone that formed due to the

welding passes and the heat affected zone located near the weld interface; these differences, formed the most brittle section of the weld joints. Figure 3B shows the microstructure of the base metal, consisting of ferrite(white area), pearlite(dark area), and bainite (slightly gray area).

The fine grain size resulted in excellent strength and toughness(Lee, 1998; Lee, 1999). Figure 3C is an optical micrograph taken from an area of the deposited weld metal, revealing the grain boundary ferrite, Widmanstatten side plate, and acicular ferrite. To improve mechanical properties such as tensile strength and toughness, acicular ferrite has to be formed fully, mean while the grain boundary ferrite and Widmanstatten side plate should be controlled to be minimum. The grain-coarsening region is shown in Fig. 3(d). The grain-coarsening region was subjected to a peak temperature well above the Ac_3 temperature, thus promoting the coarsening of austenite grains. Because of the relatively high cooling rate and the large grain size in this region, acicular ferrite, rather than blocky ferrite formed at the grain boundaries.

Figure 4 is an optical micrograph, taken from the deposited weld metal as a function of boron content. Figure 4(a) is the microstructure of deposited weld metal welded with a 32 ppm boron content wire, and 4(b) is that of the deposited weld metal welded with 60 ppm boron content wire. The optical micrograohs revealed no significant difference between Fig. 4(a) and 4(b), except for acicular ferrite content. The volume fraction of acicular ferrite decreased as the boron content increased from 32 ppm to 60 ppm. The acicular ferrite content in the specimen of 32 ppm boron was approximately 93%, while in the specimen of 60 ppm boron was 87%. In contrast, the primary ferrite such as grain boundary ferrite and Widmanstatten side plate are increased as the boron content increased, as shown in Figs. 4(a) and 4(b).

Bonnet and Charpentier(1998) observed the effect of titanium on acicular ferrite formation. They found that the addition of titanium above 0.0045 wt-% into the weld metal was essential to form a large volume fraction of acicular ferrite.

The microstructure of deposited weld metal produced with 103 ppm boron content wire is shown in Fig. 4(c). The microstructure was significantly different from those in Figs. 4(a) and 4(b). The bainite was transformed.

Oh et al.(1998) proposed that the upper bainite

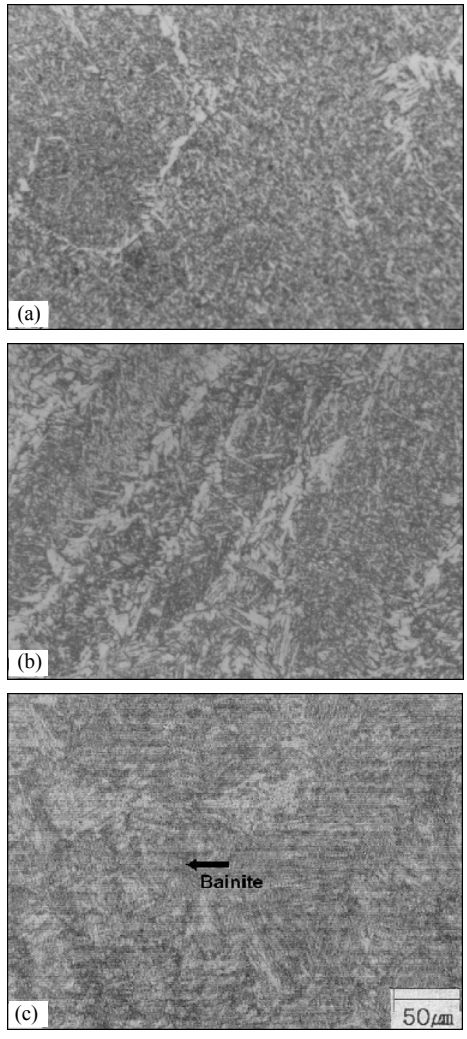

(a) 32 ppm (b) 60 ppm (c)103 ppm

Fig. 4. Microstructure of deposit metal as a function of boron content.

content increases from 0 to 8% as the boron content increases from 6 to 91 ppm. The reduction in toughness with increasing boron concentration above the optimum content can be related to the role of bainite on the degradation of weld metal properties. It is expected that variations in hardenability additions, such as manganese and carbon, will cause changes in the boron and titanium contents that achieve the optimum amount of acicular ferrite and maximum toughness.

3.2 Hardness traverses/Tensile strength

Figure 5 compares that hardness distributions in the

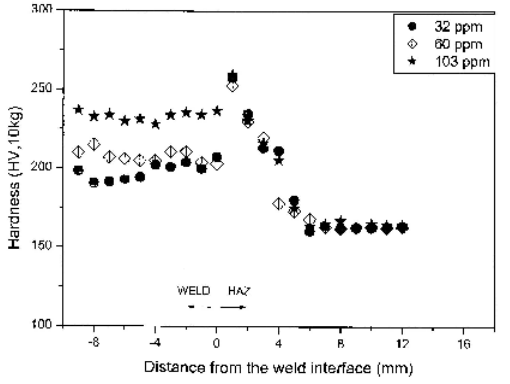

Fig. 5. Hardness traverses as a function of boron content.

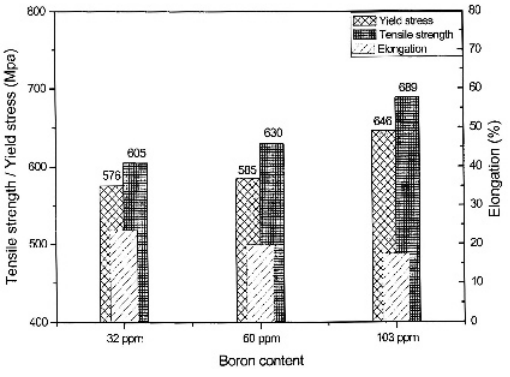

Fig. 6. Tensile/Yield strength and elongation as a function of boron content.

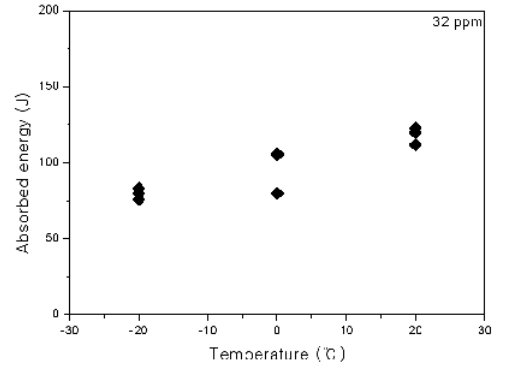

Fig. 7. Results of Charpy V-notch impact tests for 32 ppm boron content.

welds as a function of boron contents at a distance of 20 mm away from the weld surface.

The hardness values of the deposited weld metal varied significantly as a function of boron content. The hardness values welded with 32 ppm and 60 ppm boron wires ranged from Hv 190~210, while those welded with 103 ppm boron wire were in the range

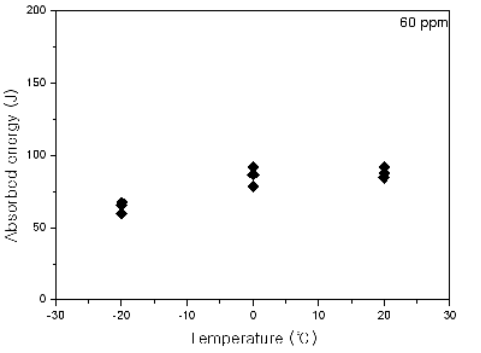

Fig. 8. Results of Charpy V-notch impact tests for 60ppm boron content.

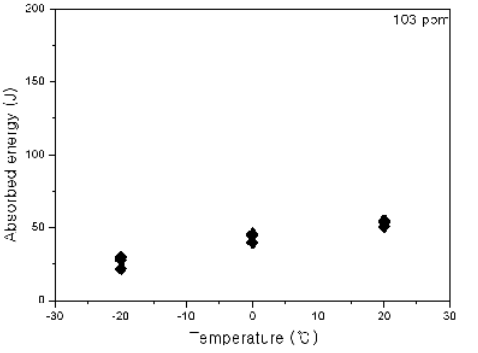

Fig. 9. Results of Charpy V-notch impact tests for 103ppm boron content.

from Hv 230~235. The hardness values increased with boron content. One suggestion for boron hardenability is the use of the fact is that free boron diffuses to the austenite grain boundaries to lower their energy, thereby making them less favorable sites for ferrite nucleation. Ohmori and Yamanaka(1979) have found evidence of grain boundary enrichment of boron with high sensitivity ion microprobe analysis.

Tensile strength, yield strength, and elongation are shown in Fig. 6 as a function of boron content. Tensile strength and yield strength increases with boron content, while elongation decreases with boron content.

3.3 Impact properties

Figures 7, 8, and 9 show the results of Charpy V-notch impact test as a function of boron content. The absorbed energy decreases with boron content. The absorbed energy slightly decreases with boron contents from 32 ppm to 60 ppm, but significantly decreases with boron contents from 60 ppm to 103

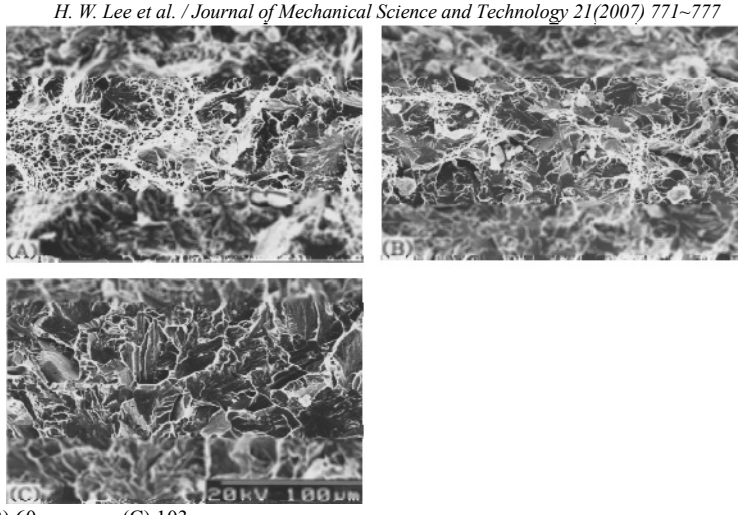

(A) 32 ppm (B) 60 ppm (C) 103 ppm
Fig. 10. SEM fractographs of impact tests at -20℃ as a function of boron content.

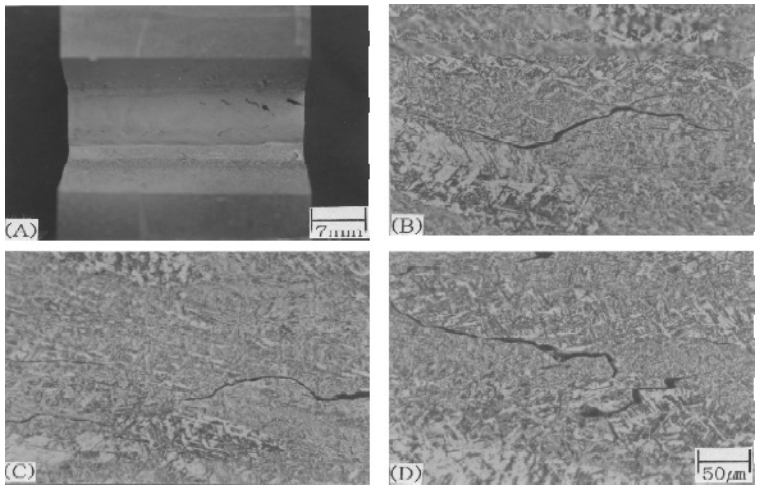

Fig. 11. Various cracks in deposited weld metal welded with 103 ppm boron content wire.

ppm.

The absorbed energies, in the specimens welded with boron contents of 32 ppm and 60 ppm wire, satisfied the specification requirement(34 J) at -20℃, while those welded with boron content of 103 ppm wire, did not satisfy the specification requirement.

Figure 10 shows the SEM fractographs of the deposited weld metal as a function of boron content after impact test at -20℃. The fracture mode changed from dimple to cleavage as the boron content increased.

3.4 Crack morphology

In the weld joint welded with 32 ppm and 60 ppm boron content electrode, no cracks were detected. However, cracks were detected the specimen welded with 103 ppm boron content electrode. This is due to bainite, susceptible microstructure to crack, which is easily transformed as increasing boron contents. Figure 11A is the results of magnetic particle inspection after 3 layers welding. The cracks were observed 45 deg to the longitudinal section. The formation of these cracks did not follow the grain, rather, they propagated the grain boundary as shown in Figure 11B, C and D.

4. Conclusions

Microstructure and mechanical properties such as,

strength, and absorbed energy were studied.

The results of this study can be summarized as follows:

(1) The volume fractions of acicular ferrite were decreased as boron contents increased from 32 to 103 ppm. The upper bainite was formed in the specimen welded with 103 ppm boron wire, while was not formed in the welds welded with wire of 32 ppm and 60 ppm boron contents.

(2) The hardness in the welds welded with 32 ppm and 60 ppm boron wires was in the range from Hv 190~210, while that welded with 103 ppm boron wire was in the range from Hv 230~235.

(3) The tensile and yield strength were increased but elongation decreased as the boron contents increased from 32 to 103 ppm.

(4) The absorbed energy was slightly decreased as boron contents increased from 32 ppm to 60 ppm, but significantly decreased as boron contents increased from 60 ppm to 103 ppm.

(5) Cracks were detected the specimen welded with 103 ppm boron content electrode, however cracks were not detected for the specimen welded with 32 ppm and 60 ppm boron content electrode.

Anowlegement

This work was supported by CANSMC from the regional innovation center(RIC) program of the ministry of commerce, industry and energy(MOCIE).

References

Babu, S. S., Goodwin, G. M., Rohde, R. J. and Sielen, B. 1998. "Effect of Boron on the Microstructure of Low-carbon Steel Resistance Seam Welds," *Welding Journal*, Vol. 77, No. 6, pp. 249~253.

Bonnet, C. and Charpentier, F. P., 1998, "Procedure of International Conference on Effect of Residual Impurity and Microalloying Elements on Weldability and Weld Properties," London, *The Welding Institute*, Abington, U.K., 8.

Brown, A., Garnish, J. D. and Honeycombe, R. W. K., 1974, "The Distribution of Boron in Pure Iron," *Metal Science* 8:317~324.

Kohno, R., Takami, T., Mori, N. and Nagano, K. 1982, "New Flux of Improved Weld Metal Toughness of HSLA Steels," *Welding Journal*, Vol. 61, No. 12, pp. 373~380.

Koukabi, A. H., North, T. H. and Bell, H. B. 1975, "Properties of Submerged arc Weld Deposits-effects of Zr,V and Ti/B," *Metal Const. and British W. J.*, 11:639.

Lee, H. W. and Kang, S. W. 1999, "Microstructure and Impact Properties of 50 mm Single Pass Electrogas Weldments for EH36 TMCP Steels," *Journal of the Korea Welding Society*, Vol. 17, No. 3, pp. 244~249.

Lee, H. W., 2006, "The Relationship Between Boron Content and Crack Properties in FCAW Deposited Metal," *Welding Journal*, Vol. 85, No. 6 pp. 131~136.

Lee, H. W., Kang, S. W. and Um, D. S., 1998, "A Study on Transverse Weld Cracks in Thick Steel Plate with the FCAW Process," *Welding Journal*, Vol. 77, No. 12, pp. 503~510.

Llewellyn, D. T. and Cook, W. T., 1974, "Metallurgy of Boron-treated Low-alloy Steels," *Metals Technology*, 12:517~529.

Maitrepierre, Ph., Thivellier, D. and Tricot, R., 1975, "Influence of Boron on the Decomposition of Austenite in Low Carbon Alloyed Steels," *Metallurgical Transactions*, 6A:287~321.

Melloy, G. F., Silmmon, P. R. and Podgursky, P. P., 1973, "Optimizing the Boron Effect," *Metallurgical Transactions*, 4:2279~2289.

Oh, D. W., Olson, D. L. and Frost, R. H., 1998, "The Influence of Boron and Titanium on Low-carbon Steel Weld Metal," *Welding Journal*, 68:151~158.

Ohmori and Yamanaka, 1979, "Procedure of International Symposium on Boron Steel," Milwaukee: 44~60.

Pargeter, R. J. and Dolby, R. E., 1985, "Guidelines for Classification of Ferritic Steel Weld Metal Microstructural Constituents Using the Light Microscope IIW Doc. IX-1377-85," *American Welding Society*, Miami, Fla.